CALPHAD and rule-of-mixtures: A comparative study for refractory high entropy alloys

Sufyan M. Shaikh [a], V.S. Hariharan [a], Satyesh K. Yadav [a], B.S. Murty [a,b,*]

[a] Department of Metallurgical and Materials Engineering, Indian Institute of Technology Madras, Tamil Nadu, 600 036, India
[b] Indian Institute of Technology Hyderabad, Telangana, 502 285, India

ARTICLE INFO

ABSTRACT

Present work studies 126 quaternary and 126 quinary equiatomic refractory high entropy alloys (RHEAs), made from Group IV (Ti, Zr, Hf), Group V (V, Nb, Ta) and Group VI (Cr, Mo, W) elements. Rule-of-mixtures (ROM) technique is used to calculate liquidus temperature, density (ρ), Young's modulus (E), % atomic size difference (δ), valence electron concentration (VEC) and specific heat at constant pressure and at 1273 K (C_p). CALPHAD technique is used to predict the number of phases formed at 298 K, ρ and liquidus temperature. ROM calculated densities are matching perfectly with CALPHAD values. Densities and E are directly proportional to the VEC and liquidus temperature of the alloys. Ti, Zr, Hf are ductilizing the alloys and making them light; whereas Cr, Mo and W, are reducing the alloys' ductility and making them heavy. For quinary RHEAs, C_p shows six distinct groups with δ, but a similar trend is not observed in quaternary RHEAs. A methodology is developed to screen a large number of alloys based on various properties. Correlations between those properties are also studied.

1. Introduction

The quest for materials sustaining high temperatures for a prolonged duration is perpetual. The demand for high-temperature alloys from aerospace and power-generation industries has increased further as they want to push the limits of their aircraft and turbines. Ni-based superalloys have ruled this application domain for the past few decades [1]. At the start of the twenty-first century, a novel alloy design strategy led to the development of a new field of alloys, called as "High Entropy Alloys (HEAs)", "Complex Concentrated Alloys (CCAs)" and "Multi-Principal Elements Alloys (MPEAs)" [2–5]. In this context, a new class of HEAs composed of refractory elements, namely, "Refractory Complex Concentrated Alloys (RCCAs)" or "Refractory High-Entropy Alloys (RHEAs)", are being actively developed as an alternative to currently used superalloys [6].

The melting point of a metal decides its end application temperature. Correspondingly, the melting point of the base metal (Ni (1728 K) or Co (1768 K)) limits the inherent strength of superalloys. Since the constituents of RHEAs are composed of refractory elements, they are expected to show better high-temperature properties. $AlMo_{0.5}NbTa_{0.5}TiZr$ is one such RHEA which has a yield strength of 1597 MPa at 1073 K, whereas, that of TMS-238 (6th gen. superalloy) is 1041 MPa at 1023 K [7,8]. The

superior yield strength value shows the immense potential of RHEAs for high-temperature applications. Among the RHEAs synthesised so far, MoNbTaW (3177 K) and MoNbTaWV (2946 K) possess very high liquidus temperatures [9]. The liquidus temperature is estimated using ROM as there is a lack of experimental data [9]. High liquidus temperature makes the property determination of RHEAs difficult, given the fact that not all the characterisation equipment can sustain high temperatures for a prolonged duration. Accurate determination of high-temperature mechanical properties of RHEAs remain a challenge as their liquidus temperature is higher than that of the superalloy clamps used in the high-temperature tensile/compression testing machines.

Material development for any specific application demands one to study a large number of alloys and their properties. As mentioned earlier, if the alloys being developed are RHEAs, then their property determination becomes quite challenging. Most of the studied RHEAs are either quaternary or quinary alloys starting from the seminal work of Senkov et al. in 2010 [9,10]. Thus, the current work is focused on quaternary and quinary equiatomic RHEAs. The present report proposes a methodology to study a large number of alloy families, which does not require heavy computational resources. Various properties like liquidus temperature, density are calculated using rule-of-mixtures (ROM) relations and compared with CALculation of PHase Diagram (CALPHAD)

Table 1

Relations used for property estimation. r_i: radius of individual element's atom, $\bar{r}$: avg. atomic radius of alloy, C: atom fraction, A: atomic weight (g/mol), ρ: density (g/cc), V: molar volume (m³), C_p: specific heat at constant pressure at 1273.

Property	Formula
Density (g/cc)	$\rho_{alloy} = \dfrac{\sum_i (C \cdot A)_i}{\sum_i \left(\dfrac{C \cdot A}{\rho}\right)_i}$
Young's Modulus (GPa)	$E_{alloy} = \dfrac{\sum_i (C \cdot V \cdot E)_i}{\sum_i (C \cdot V)_i}$
%Radius mismatch/atomic size difference	$\delta = \sqrt{\sum_i C_i \cdot \left(1 - \dfrac{r_i}{\bar{r}}\right)^2}$
Valence Electron Concentration	$VEC = \sum_i C_i \cdot Valency_i$
Melting Point/Liquidus (K)	$T_m = \sum_i C_i \cdot T_i$
Specific heat at 1273 K (J/mol.K)	$C_p = \sum_i (C_p \cdot T)_i$

approach. In addition, the proposed technique can quickly narrow down the alloy family depending upon requirements.

2. Methods

Alloy combinations are selected from a palette of nine elements from Group-IV (Ti, Zr, Hf), Group-V (V, Nb, Ta) and Group-VI (Cr, Mo, W). A total of 126 ($_9C_4$) quaternary (4RHEA) and 126 ($_9C_5$) quinary (5RHEA) equiatomic RHEAs have been studied. Density (ρ), Young's Modulus (E), valence electron concentration (VEC), liquidus temperature, % atomic size difference (δ) and specific heat at constant pressure at 1273 K (C_p) of 4RHEA and 5RHEA are calculated with the help of rule-of-mixtures (ROM) relations given in Table 1 [11,12].

The values of individual elements are taken from Refs. [13,14]. For the CALPHAD approach, Thermo-Calc software with TCHEA (v2.1) database is used to predict overall alloy density (ρ), number of phases (at 298 K) and liquidus temperatures of the respective alloys [15].

Calculated properties are first plotted in the form of a scatter matrix plot, and then their respective "Pearson's r parameter"/correlation parameter is calculated and analysed. Figures with additional information are included in the supplementary data.

3. Results

3.1. Density, liquidus temperature

Fig. 1(a) and (b) shows the ROM estimated density (Density-ROM) and CALPHAD calculated density (Density-TC) of the 4RHEAs and 5RHEAs, respectively. Alloys with the lowest density are TiZrVCr (6.03 g/cm³) and TiZrVCrNb (6.57 g/cm³), whereas, the heaviest are MoTaWHf (14.81 g/cm³) and MoTaWHfCr (13.72 g/cm³). Table 2 [9, 16–19] compares ROM and CALPHAD calculated density values with experimental densities of a few equiatomic RHEAs available in the literature. It is important to note that the ROM densities are very close to

Table 2

Experimental, ROM and CALPHAD calculated densities (ρ) of few equiatomic RHEAs.

| S. No.	Alloy	Experimental ρ (g/cm³)	ROM ρ (g/cm³)	CALPHAD ρ (g/cm³)	Reference (for experimental ρ)
			Present work		
1	MoNbTaW	13.64	13.75	13.8	[9]
2	MoNbTaWV	12.36	12.36	12.44	[9]
3	NbTiVZr	6.52	6.5	6.4	[16]
4	CrNbTiZr	6.67	6.7	6.73	[16]
5	CrNbTiVZr	6.57	6.52	6.68	[16]
6	TiZrHfNbTa	9.94	9.91	9.89	[17]
7	TiZrHfMoTa	10.24	10.21	10.19	[18]
8	MoNbTaTiW	11.72	11.76	11.85	[19]
9	NbTiZrVMo	7.27	7.13	7.18	[19]
10	NbTiZrVTa	8.43	8.5	8.5	[19]
11	NbTiZrVCr	6.57	6.57	6.68	[19]
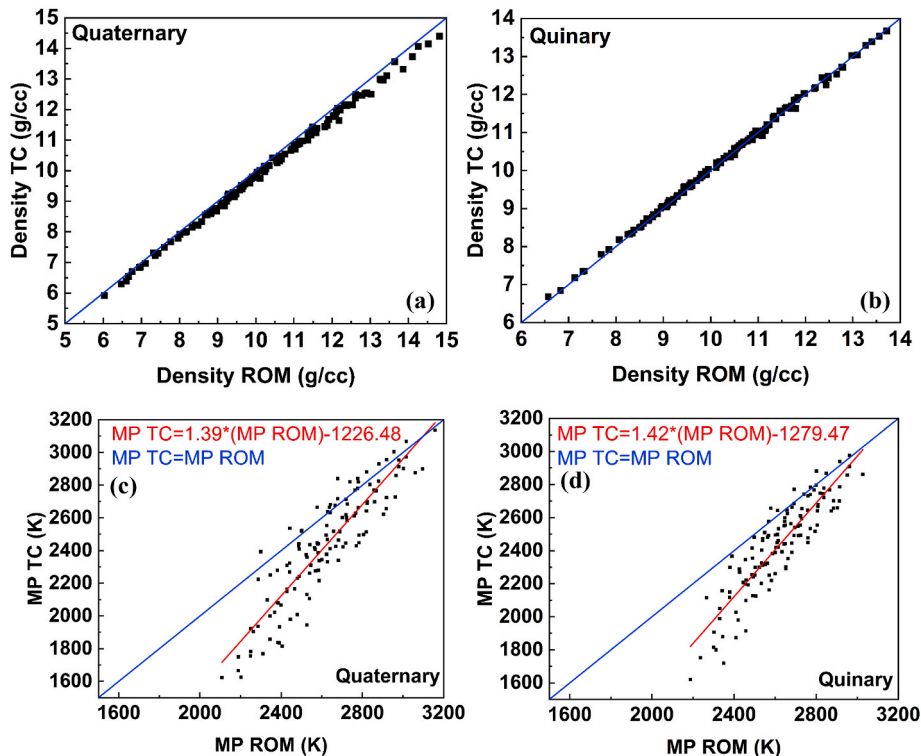
Fig. 1. Density comparison of (a) 4RHEA (b) 5RHEA, by ROM and CALPHAD. Melting point comparison of (c) 4RHEA (d) 5RHEA, by ROM and CALPHAD.
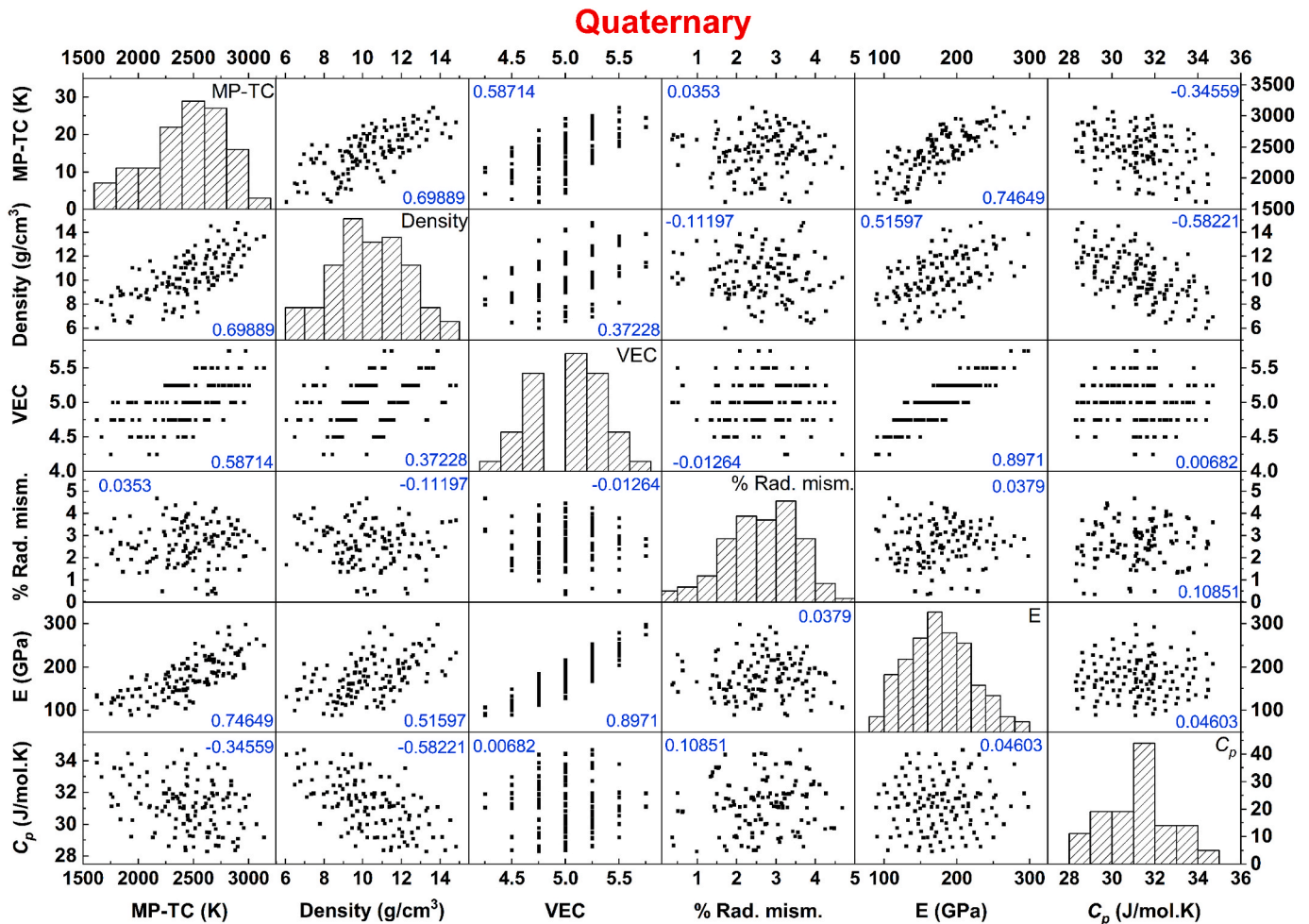
Fig. 2. Overview of relationships between different properties for 4RHEA. Numbers in blue colour inside each graph are "Pearson's r" parameter.

the experimentally determined values. Fig. 1(c) and (d) shows the ROM calculated liquidus temperature (MP-ROM) and CALPHAD calculated liquidus temperature (MP-TC) of the 4RHEA and 5RHEA, respectively. Alloys with the lowest liquidus temperature are, TiZrVCr (MP-ROM = 2108 K, MP-TC = 1623 K) and TiZrVCrHf (MP-ROM = 2187 K, MP-TC = 1621 K), whereas, MoNbTaW (MP-ROM = 3158 K, MP-TC = 3138 K) and MoNbTaWV (MP-ROM = 2963 K, MP-TC = 2976 K) have the highest liquidus temperature.

From Figs. 2 and 3, for both the alloy families, it is clear that the density is reasonably correlated with the MP-TC, as indicated by 0.69 correlation factor (number in blue colour). Figs. S1(a) and (b) (of supplementary data) show four distinct groups for 4RHEAs and 5RHEAs, respectively. In each of these groups, the density increases with VEC, as shown by the positive slope of the trend lines in Fig. S1. The alloys have more amount of Group-VI (Cr, Mo, W) elements as we move further towards the top right side of the graph, on the other hand, at the bottom left of the graph, the alloys have more amount of Group-IV (Ti, Zr, Hf) elements (Fig. S1).

3.2. Young's modulus

Young's Modulus (E) is strongly correlated with MP-TC, ρ and VEC for both 4RHEAs and 5RHEAs (Figs. 2, 3 and Fig. S2 of supplementary data). They are explained in the next two sections.

3.2.1. 4RHEAs
In 4RHEAs, TiZrHfNb (89.37 GPa) has the lowest E value, whereas,

TaCrMoW (298.23 GPa) has the highest E value. For 4RHEAs, E shows 0.75 correlation with MP-TC, 0.52 correlation with density and 0.90 correlation with VEC (Fig. 2). According to the VEC = 4.5 threshold [20], TiZrHfTa, TiZrVTa and TiZrHfV are estimated to possess good ductility among the studied alloys whereas, CrMoWTa, CrMoWNb and CrMoWNb alloys are estimated to possess poor ductility among the studied alloys (Fig. S1(a) of supplementary data). E vs. density plot shows four distinct groups (Fig. S2(a) of supplementary data). From S2 (a), majority of the alloys in the group (1) have Ti, Zr and Hf, whereas, majority of the alloys in the group (4) have Cr, Mo and W.

3.2.2. 5HREAs
In 5RHEAs, TiZrHfNbV (94.99 GPa) has the lowest E value, whereas, TaCrMoWV (266.93 GPa) has the highest E value. For 5RHEAs, E shows 0.76 correlation with MP-TC, 0.51 correlation with density and 0.90 correlation with VEC (Fig. 3). According to the VEC = 4.5 threshold [20], TiZrHfTaNb, TiZrHfVTa and TiZrHfVNb alloys have good ductility among the studied alloys. In contrast, CrMoWNbTa, CrMoWVTa and VCrMoWNb alloys have poor ductility among the studied alloys as indicated in Fig. S2(b). From S2(b) of supplementary data, majority of the alloys in the group (1) have Ti, Zr and Hf, whereas, majority of the alloys in the group (4) have Cr, Mo and W.

3.3. Specific heat at constant pressure and at 1273 K (C_p)

In 4RHEAs, C_p shows a weak correlation of about −0.35 with MP-TC and a strong correlation of about −0.58 with ρ (Fig. 2). Similarly, in 5RHEAs, C_p shows a weak correlation of about −0.31 with MP-TC and a
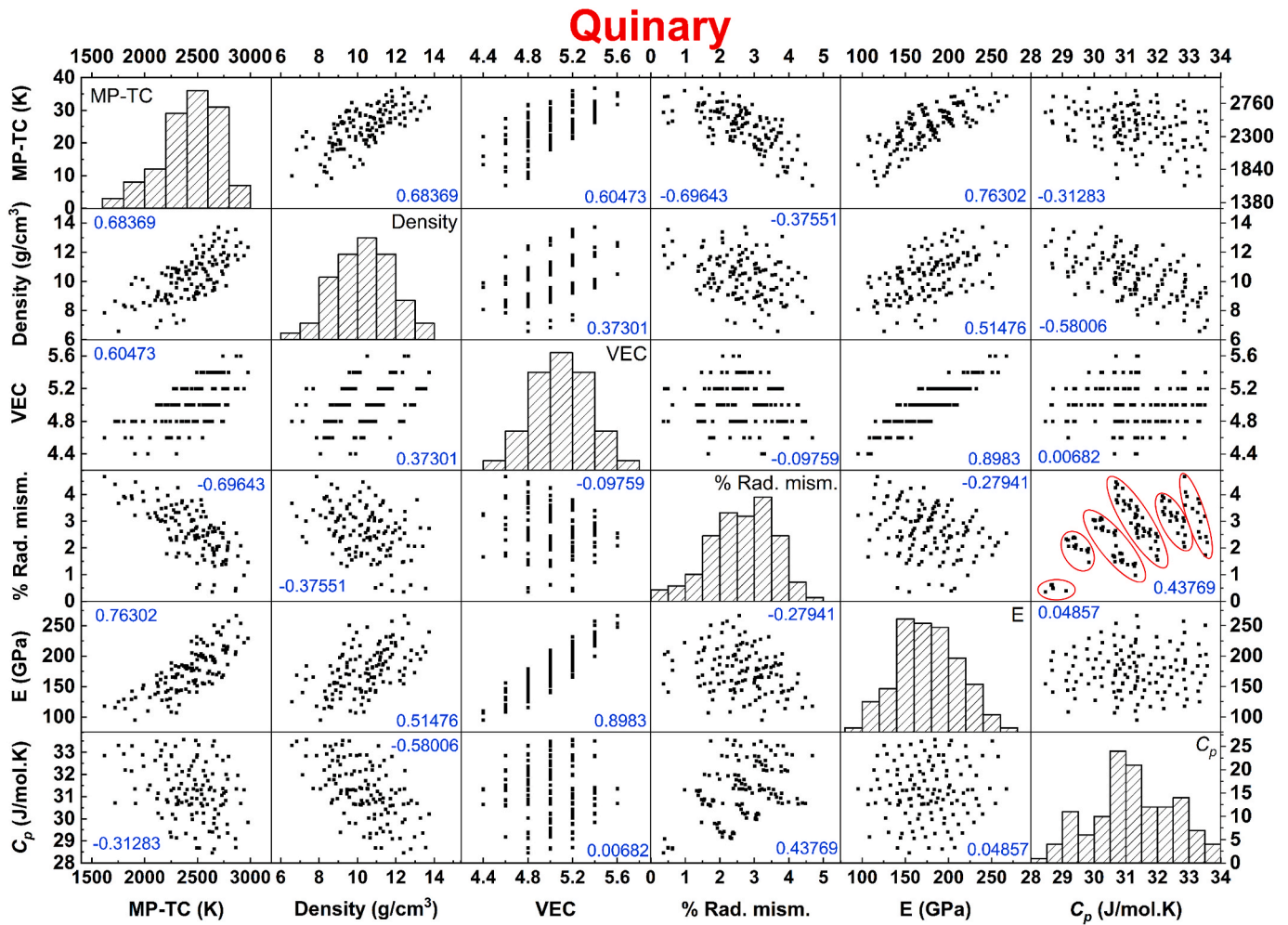
Fig. 3. Overview of relationships between different properties for 5RHEA. Numbers in blue colour inside each graph are "Pearson's r" parameter.

strong correlation of about −0.58 with ρ (Fig. 3). In 5RHEAs, C_p shows six distinct groups with % atomic size difference (red circles Fig. 3). However, a similar trend is not observed in 4RHEAs.

3.4. Phases

3.4.1. 4RHEAs

Fig. 4(a) shows the number of phases present at 298 K for 4RHEAs. While only one alloy (MoNbTaW) has single-phase, 40 alloys have two-phase, 71 alloys have three-phase, and 14 alloys have four-phase microstructure. There is no five-phase microstructure alloy in 4RHEAs. Majority of 4RHEAs have three-phase microstructure. These alloys have a relatively high occurrence of Zr, Hf and Nb as compared to other elements (Fig. 4(b)). Most of the four-phase 4RHEAs are composed of Ti and Ta (Fig. 4(b)).

3.4.2. 5RHEAs

Fig. 4(c) shows the number of phases present at 298 K for 5RHEAs. Eighteen alloys have two-phase, 84 alloys have three-phases, 23 alloys have four-phase, and only one alloy (TiVTaCrMo) has five-phase microstructure. It is interesting to note that there is no single-phase alloy in 5RHEAs unlike 4RHEAs. Majority of 5RHEAs have three-phase microstructure having similar occurrence of all the nine elements (Fig. 4(d)). Most of the four-phase 5RHEAs are composed of Ti, Zr and Hf (Fig. 4(d)).

3.5. VEC analysis

Fig. 4(e) and (f) show the occurrence of all the constituent elements in 4RHEA and 5RHEA of different VEC values, respectively. Alloys can be made ductile by decreasing their VEC values with the help of appropriate alloying elements [21]. The criteria for good ductility (VEC < 4.5) is taken from Refs. [20–22]. Accordingly, among the studied 4RHEAs and 5RHEAs, Ti, Zr, Hf containing alloys are expected to show high ductility, whereas, Cr, Mo, W containing alloys are expected to show low ductility.

Fig. S1 of supplementary data compares density with VEC. The boundary between ductile and brittle alloy is taken at VEC = 4.5 [20]. From Fig. S1(a) (of supplementary data), it can be seen that among the studied 4RHEAs, TiZrHfV, TiZrHfNb, TiZrHfTa are expected to show high ductility (VEC = 4.25); and, TaCrMoW, NbCrMoW, VCrMoW are expected to show low ductility (VEC = 5.75). From S1(b) (of supplementary data), it is evident that among the studied 5RHEAs, TiZrHfVNb, TiZrHfVTa, TiZrHfNbTa can show high ductility (VEC = 4.4); and NbTaCrMoW, VTaCrMoW, VNbCrMoW can show low ductility (VEC = 5.6). These results are in line with earlier studies on TiZrHfNbTa and TiZrHfMoTa alloy, which have shown them to have excellent strength and ductility combination [17,18,23–25].

4. Discussion

The overall alloy density calculated using CALPHAD approach and ROM technique is similar, as observed from Fig. 1(a) and (b). In
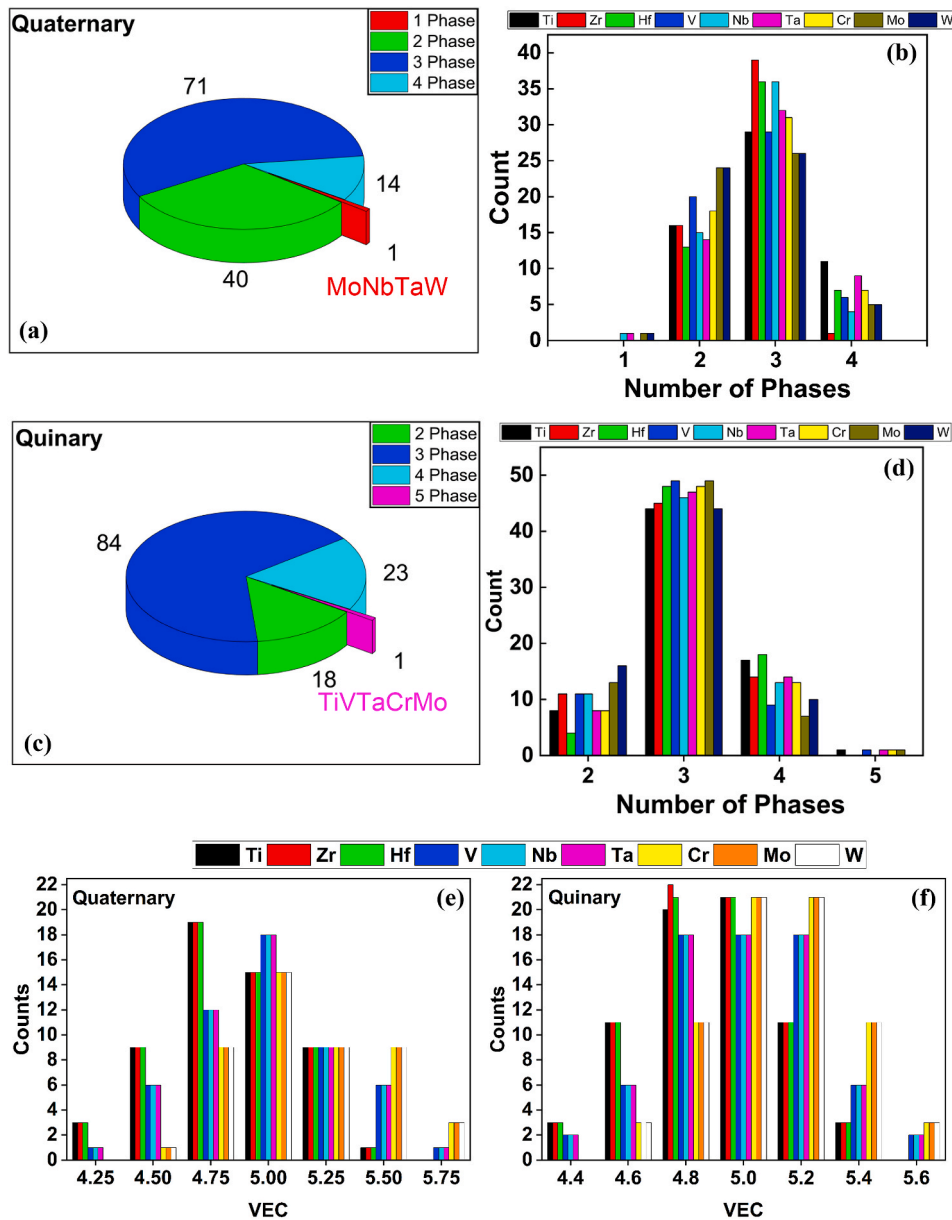
Fig. 4. (a) Overview of number of phases in 4RHEA. (b) Occurrence of elements in 1/2/3/4 phases in 4RHEA. (c) Overview of number of phases in 5RHEA. (d) Occurrence of elements in 2/3/4/5 phases in 5RHEA. Occurrence of respective elements in various (e) 4RHEA and (f) 5RHEA of different VEC values.

addition, Table 2 indicates that the ROM calculated densities are very close to experimentally measured values in the cases considered. Therefore, the density can be estimated with reasonably good accuracy using ROM. Experimental determination of the liquidus temperature is challenging due to the extremely high melting points of RHEAs. Based on the literature survey, there is no report which gives experimentally determined liquidus temperature for RHEAs. Therefore, CALPHAD technique is used to estimate the liquidus temperature. The ROM estimated liquidus temperatures have shown significant deviations from CALPHAD calculated values at lower temperature ranges (Fig. 1(c) and (d)). This is because the ROM technique does not take into account the interactions among the elements, whereas CALPHAD has a thermodynamic basis and considers interaction between the elements.

As the VEC of alloys increases, their ρ and E also increase (Figs. 2, 3, S1 and S2), pointing to the fact that increase in VEC is facilitating the reduction of molar volume. The relationship between VEC and molar volume can be explained from the trend observed in the periodic table. In the periodic table, as we move across periods from Group-IV (Ti, Zr,

Hf) to Group-VI (Cr, Mo, W), the number of electrons (valency) and protons in the atom increases. The increased positive charge on the nucleus decreases the overall atomic size of the atom by attracting the electron cloud towards it. Decreased atomic size reduces the molar volume of the element. Increased VEC leads to an overall reduction in the average atomic size of the alloy, which in turn reduces the molar volume. Reduced molar volume, combined with heavy elements, increase the ρ of alloys.

Thus, with higher fraction of Group VI constituents in comparison to Group IV leads to an increase in VEC of the alloy, which leads to a decrease in average alloy atomic size, which in turn decreases the molar volume of the alloy. In addition, a higher fraction of Group VI elements in the alloy also increases the average alloy atomic weight and hence the density of the alloy increases. Similarly, as the VEC increases, the average alloy bond strength increases, which leads to higher liquidus temperature and increased Young's modulus (Figs. 2 and 3).

For alloys to be ductile, the dislocation nucleation should occur before crack nucleation. Dislocation nucleates when the local shear

stress on the slip plane becomes equal to the ideal shear strength. Whereas, crack initiates when the tensile stress on the direction perpendicular to the cleavage plane exceeds tensile strength [26]. However, some alloys fail by shear deformation without any cracking even when they are loaded in tensile mode on the direction perpendicular to cleavage plane [27]. This is known as "shear instability", where the dislocations get activated before cracking, and the materials become intrinsically ductile. Alloy becomes intrinsically brittle when shear instability occurs after the tensile strength is reached. Mo and W are two such examples of intrinsically brittle metals, which have been made ductile by decreasing their VEC (by alloying), which leads to Jahn-Teller distortion [22]. A similar concept has been used to ductilize high entropy alloys by decreasing their VEC with appropriate alloying additions [20,21].

Alloying with low valency elements can lead to the development of intrinsic ductility in RHEAs. In present work, Ti, Zr and Hf have the lowest valency among the elements. Therefore, addition of Ti, Zr and Hf can help in ductilizing the RHEAs (Fig. 4(e), (f)) by reducing the overall VEC of the alloy. Similarly, addition of Cr, Mo and W can make the RHEA brittle by increasing the overall VEC of the alloy (Fig. 4(e) and (f)).

From Fig. S2, for both 4RHEAs and 5RHEAs, the alloy can be made ductile and light by using relatively light elements such as Ti, Zr and Hf which reduces the VEC to below 4.5 threshold [20]. Similarly, the alloy can be made stronger and heavy by using relatively heavy elements such as Cr, Mo and W, which increases the VEC to way above 4.5 threshold [20].

Fig. 4(a) and (c) indicate that the high entropy effect is not helping the alloy to solidify in a single phase. Except one alloy (MoNbTaW), the rest of the 4RHEAs and 5RHEAs are multi-phase alloys which suggests that not only entropy of mixing but also the enthalpy of mixing should be taken into account while defining the phase formation criteria [16, 28]. In 4RHEAs while Zr, Hf and Nb help the alloys to solidify in a three-phase microstructure, Ti and Ta help them to solidify in a four-phase microstructure (Fig. 4(b)). In 5RHEAs, Ti, Zr and Hf are helping the alloys to solidify in a four-phase microstructure. The majority of 4RHEAs and 5RHEAs are predicted to have three-phase microstructures (Fig. 4(b) and (d)) at room temperature.

The scatter matrix plots shown in Figs. 2 and 3 give an overview of various properties and their inter-relations for 4RHEAs and 5RHEAs, respectively. In two figures, 252 different alloy families are studied on six different parameters (Figs. 2 and 3). This approach helps in screening alloys based on application and design requirements, as shown in S1 and S2 (of supplementary data). The "scatter-matrix-plot" approach quantifies all the possible combinations between various properties in the form of correlation parameter (blue numbers in Figs. 2 and 3).

5. Conclusions

In summary, we have studied all possible equiatomic quaternary and quinary RHEAs made from Group-IV (Ti, Zr, Hf), Group-V (V, Nb, Ta) and Group-VI (Cr, Mo, W) elements. Correlations between liquidus temperature, density, VEC, atomic size difference, C_p and E have been studied for 252 different RHEA families. While the anomaly for C_p in 5RHEAs needs further extensive evaluation, the present work shows that ROM complemented with CALPHAD technique can act as a useful tool to study a large number of alloy families, without requiring heavy computational resources.

The "scatter-matrix-plot" methodology can help alloy designers screen a large number of alloy systems. It will also help them narrow down alloy family depending upon application requirements. Those requirements can be different ranges of liquidus temperature, density, Young's modulus or specific modulus. It will also help them decide weightage to different properties according to their design and application requirements.

CRediT authorship contribution statement

Sufyan M. Shaikh: Conceptualization, Methodology, Software, Validation, Formal analysis, Investigation, Data curation, Writing - original draft, Visualization. **V.S. Hariharan:** Methodology, Software, Data curation, Writing - review & editing. **Satyesh K. Yadav:** Resources, Writing - review & editing. **B.S. Murty:** Resources, Writing - review & editing, Supervision, Project administration.

Declaration of competing interest

The authors declare that they have no known competing financial interests or personal relationships that could have appeared to influence the work reported in this paper.

Acknowledgements

Appendix A. Supplementary data

Supplementary data to this article can be found online at https://doi.org/10.1016/j.intermet.2020.106926.

References

[1] R.C. Reed, The Superalloys, Cambridge University Press, Cambridge, 2006, https://doi.org/10.1017/CBO9780511541285.

[2] S. Ranganathan, Alloyed pleasures: multimetallic cocktails, Curr. Sci. 85 (2003) 1404–1406.

[3] J.W. Yeh, S.K. Chen, S.J. Lin, J.Y. Gan, T.S. Chin, T.T. Shun, C.H. Tsau, S.Y. Chang, Nanostructured high-entropy alloys with multiple principal elements: novel alloy design concepts and outcomes, Adv. Eng. Mater. 6 (2004) 299–303+274.

[4] D.B. Miracle, J.D. Miller, O.N. Senkov, C. Woodward, M.D. Uchic, J. Tiley, Exploration and development of high entropy alloys for structural applications, Entropy 16 (2014) 494–525, https://doi.org/10.3390/e16010494.

[5] B.S. Murty, J.W. Yeh, S. Ranganathan, P.P. Bhattacharjee, High-Entropy Alloys, second ed., Elsevier, 2019. https://www.elsevier.com/books/high-entropy-alloys/murty/978-0-12-816067-1.

[6] O.N. Senkov, G.B. Wilks, J.M. Scott, D.B. Miracle, Mechanical properties of Nb$_{25}$Mo$_{25}$Ta$_{25}$W$_{25}$ and V$_{20}$Nb$_{20}$Mo$_{20}$Ta$_{20}$W$_{20}$ refractory high entropy alloys, Intermetallics 19 (2011) 698–706. https://www.elsevier.com/books/high-entropy-alloys/murty/978-0-12-816067-1.

[7] O.N. Senkov, S.V. Senkova, C. Woodward, Effect of aluminum on the microstructure and properties of two refractory high-entropy alloys, Acta Mater. 68 (2014) 214–228, https://doi.org/10.1016/j.actamat.2014.01.029.

[8] K. Kawagishi, A.-C. Yeh, T. Yokokawa, T. Kobayashi, Y. Koizumi, H. Harada, Development of an oxidation-resistant high-strength sixth-generation single-crystal superalloy TMS-238, in: Superalloys 2012, John Wiley & Sons, Inc., Hoboken, NJ, USA, 2012, pp. 189–195, https://doi.org/10.1002/9781118516430.ch21.

[9] O.N. Senkov, G.B. Wilks, D.B. Miracle, C.P. Chuang, P.K. Liaw, Refractory high-entropy alloys, Intermetallics 18 (2010) 1758–1765, https://doi.org/10.1016/j.intermet.2010.05.014.

[10] S. Gorsse, M.H. Nguyen, O.N. Senkov, D.B. Miracle, Database on the mechanical properties of high entropy alloys and complex concentrated alloys, Data Br 21 (2018) 2664–2678, https://doi.org/10.1016/j.dib.2018.11.111.

[11] D.B. Miracle, O.N. Senkov, A critical review of high entropy alloys and related concepts, Acta Mater. (2017), https://doi.org/10.1016/j.actamat.2016.08.081.

[12] H. Kopp III., Investigations of the specific heat of solid bodies, Phil. Trans. Roy. Soc. Lond. 155 (1865) 71–202, https://doi.org/10.1098/rstl.1865.0003.

[13] W.F. Gale, T.C. Totemeier, Smithells Metals Reference Book, eighth ed., Elsevier, 2003 https://doi.org/10.5860/choice.42-1588.

[14] M.W. Chase Jr., NIST-JANAF Thermochemical Tables, American Institue of Physics and American Chemical Society, Fourth, 1998. https://srd.nist.gov/JPCRD/jpcrdM9.pdf.

[15] H.L. Chen, H. Mao, Q. Chen, Database development and Calphad calculations for high entropy alloys: challenges, strategies, and tips, Mater. Chem. Phys. 210 (2018) 279–290, https://doi.org/10.1016/j.matchemphys.2017.07.082.

[16] O.N. Senkov, S.V. Senkova, C. Woodward, D.B. Miracle, Low-density, refractory multi-principal element alloys of the Cr-Nb-Ti-V-Zr system: microstructure and phase analysis, Acta Mater. 61 (2013) 1545–1557, https://doi.org/10.1016/j.actamat.2012.11.032.

[17] O.N. Senkov, J.M. Scott, S.V. Senkova, F. Meisenkothen, D.B. Miracle, C. F. Woodward, Microstructure and elevated temperature properties of a refractory TaNbHfZrTi alloy, J. Mater. Sci. 47 (2012) 4062–4074, https://doi.org/10.1007/s10853-012-6260-2.

[18] C.C. Juan, M.H. Tsai, C.W. Tsai, C.M. Lin, W.R. Wang, C.C. Yang, S.K. Chen, S. J. Lin, J.W. Yeh, Enhanced mechanical properties of HfMoTaTiZr and HfMoNbTaTiZr refractory high-entropy alloys, Intermetallics 62 (2015) 76–83, https://doi.org/10.1016/j.intermet.2015.03.013.

[19] O.N. Senkov, S. Rao, K.J. Chaput, C. Woodward, Compositional effect on microstructure and properties of NbTiZr-based complex concentrated alloys, Acta Mater. 151 (2018) 201–215, https://doi.org/10.1016/j.actamat.2018.03.065.

[20] S. Sheikh, S. Shafeie, Q. Hu, J. Ahlström, C. Persson, J. Veselý, J. Zýka, U. Klement, S. Guo, Alloy design for intrinsically ductile refractory high-entropy alloys, J. Appl. Phys. 120 (2016), https://doi.org/10.1063/1.4966659, 164902.

[21] T. Yang, Y.L. Zhao, W.H. Liu, J.H. Zhu, J.J. Kai, C.T. Liu, Ductilizing brittle high-entropy alloys via tailoring valence electron concentrations of precipitates by controlled elemental partitioning, Mater. Res. Lett. 6 (2018) 600–606, https://doi.org/10.1080/21663831.2018.1518276.

[22] H.A. Jahn, E. Teller, Stability of polyatomic molecules in degenerate electronic states I. Orbital degeneracy, Appl. Gr. Theory. (1968) 233–255, https://doi.org/10.1016/b978-0-08-203190-1.50014-7.

[23] O.N. Senkov, S.L. Semiatin, Microstructure and properties of a refractory high-entropy alloy after cold working, J. Alloys Compd. 649 (2015) 1110–1123, https://doi.org/10.1016/j.jallcom.2015.07.209.

[24] L. Lilensten, J.P. Couzinié, L. Perrière, A. Hocini, C. Keller, G. Dirras, I. Guillot, Study of a bcc multi-principal element alloy: tensile and simple shear properties and underlying deformation mechanisms, Acta Mater. 142 (2018) 131–141, https://doi.org/10.1016/j.actamat.2017.09.062.

[25] C.C. Juan, M.H. Tsai, C.W. Tsai, W.L. Hsu, C.M. Lin, S.K. Chen, S.J. Lin, J.W. Yeh, Simultaneously increasing the strength and ductility of a refractory high-entropy alloy via grain refining, Mater. Lett. 184 (2016) 200–203, https://doi.org/10.1016/j.matlet.2016.08.060.

[26] A. Kelly, N.H. Macmillan, Strong Solids, Clarendon Press, 1986. https://www.google.co.in/books/edition/Strong_Solids/z5NRAAAAMAAJ?hl=en&gbpv=0&bsq=A.%20Kelly,%20N.H.%20Macmillan%20Strong%20Solids,%20Clarendon%20Press,%201986.

[27] J.W. Morris, C.R. Krenn, The internal stability of an elastic solid, Philos. Mag. A 80 (2000) 2827–2840, https://doi.org/10.1080/01418610008223897.

[28] O.N. Senkov, J.D. Miller, D.B. Miracle, C. Woodward, Accelerated exploration of multi-principal element alloys with solid solution phases, Nat. Commun. 6 (2015) 1–10, https://doi.org/10.1038/ncomms7529.